land

MDPI

Article

Distribution, Risk Assessment and Source Identification of Potentially Toxic Elements in Coal Mining Contaminated Soils of Makarwal, Pakistan: Environmental and Human Health Outcomes

Liaqat Ali [1], Shehzad Ali [1,*], Seema Anjum Khattak [1], Hammad Tariq Janjuhah [2], George Kontakiotis [3], Rahib Hussain [1,4], Shah Rukh [1], Mohammad Tahir Shah [1], George D. Bathrellos [5,*] and Hariklia D. Skilodimou [6]

[1] National Centre of Excellence in Geology, University of Peshawar, Peshawar 25130, Pakistan; liaqat.nceg@uop.edu.pk (L.A.); s_anjum@uop.edu.pk (S.A.K.); rahib.cees@pu.edu.pk (R.H.); shahrukh.nceg@uop.edu.pk (S.R.); tahir_shah@uop.edu.pk (M.T.S.)
[2] Department of Geology, Shaheed Benazir Bhutto University, Sheringal 18050, Pakistan; hammad@sbbu.edu.pk
[3] Department of Historical Geology-Paleontology, Faculty of Geology and Geoenvironment, School of Earth Sciences, National and Kapodistrian University of Athens, Panepistimiopolis, Zografou, 15784 Athens, Greece; gkontak@geol.uoa.gr
[4] College of Earth and Environmental Sciences, University of the Punjab, Lahore 54590, Pakistan
[5] Sector of General, Marine Geology & Geodynamics, Department of Geology, University of Patras, Rio, 26504 Patras, Greece
[6] Department of Geology, University of Patras, 26504 Patras, Greece
* Correspondence: sali9250@gmail.com (S.A.); gbathrellos@upatras.gr (G.D.B.)

check for updates

Citation: Ali, L.; Ali, S.; Khattak, S.A.; Janjuhah, H.T.; Kontakiotis, G.; Hussain, R.; Rukh, S.; Shah, M.T.; Bathrellos, G.D.; Skilodimou, H.D. Distribution, Risk Assessment and Source Identification of Potentially Toxic Elements in Coal Mining Contaminated Soils of Makarwal, Pakistan: Environmental and Human Health Outcomes. *Land* **2023**, *12*, 821. https://doi.org/10.3390/land12040821

Academic Editors: Evangelia Golia, Vassilios Diakoloukas and Nikolaos Tsiropoulos

Received: 13 March 2023
Revised: 30 March 2023
Accepted: 31 March 2023
Published: 3 April 2023

Copyright: © 2023 by the authors. Licensee MDPI, Basel, Switzerland. This article is an open access article distributed under the terms and conditions of the Creative Commons Attribution (CC BY) license (https://creativecommons.org/licenses/by/4.0/).

Abstract: The present research was carried out to examine the health and environmental impacts associated with coal mining activities in the Makarwal coal mining area in Pakistan. To achieve the objectives, 41 soil samples were collected from the coalmine-affected areas and analyzed for major and toxic trace elements (TTEs) using atomic absorption spectroscopy. Most of the soil samples have extremely high concentrations of toxic metals such as Ni, Cd, Cr, Cu, Zn, and Pb. The positive correlations and high concentration of trace elements in the Makarwal coalmine-affected region suggest an analogous origin of soil contamination. The factor analysis (FA) showed two components, i.e., F1 (53.4%) and F (74.21%), of total variability for soil. The F2 was loaded with Pb, Zn, Ni, and Cr, which was similar to cluster 2, while the F1 was loaded with Cu and Cr, having a similar pattern to cluster 1. This proves that the contamination in the surrounding area is mostly associated with geological ore strata existing in the Makarwal coalfield. Based on geoaccumulation (I_{geo}), the elemental concentration in the studied soil sample could be categorized as follows: (1) Pb, Ni, and Zn are moderate to severely polluted and (2) Cr and Cu are in the moderately polluted category. The ecological risk indices (ERIs) of the single trace element contamination index highlighted that Cd, Pb, Ni, and Cr pose a high risk to humans and the ecosystem. Based on different statistical tools performed for the source identification and distribution of metal contamination, it seems that the exposed sedimentary rocks, including limestone, dolomite, sandstone, and coal, are responsible for the toxic metal contamination in the study area.

Keywords: coalfield; ecological risk mapping; geostatistics; health risk; pollution indices; TTEs

1. Introduction

Coal is the main source of energy and has been thought of as the economic backbone of the country for a long time. However, the coalmine's health and environmental consequences must not be overlooked [1–4]. Up to 76 of the 92 elements are found naturally in coal. The elements that have a high concentration as well as an economic importance are called "critical", while the elements that have a lower concentration than 100 mg/kg

or Earth crust abundance are called "trace" elements [5]. In fact, due to their lower cut-off grade value, the critical elements can be considered hazardous if their concentration exceeds the permissible limits. Coalmines release toxic and trace elements through local dumping, coal burning, fly ash deposition, coalmine drainage, smoke, and coal ash deposition, which may trigger environmental pollution [6]. Acid mines can have a big impact on the drainage system in coal mining areas. This is because the pyrite (iron sulfide) in the coal reacts with water and air to make acidic water, which dissolves and moves metal from the adjacent rocks [7]. Further, coal mining can generate huge quantities of solid waste due to overburden dumping, loading and unloading, and rainfall. However, coal cleaning plants may release a huge amount of coal slime, coal gangue, and liquid wastes.

Soil is the primary pool for pollutants and biota, where elemental pollutants can be transferred to living organisms, groundwater, food crops, and the nearby environment [8–11]. Soil has a natural elemental and nutrient concentration associated with its parent materials, but the boosted elemental content is because of mining (coal mining, copper mining) and other human activities, i.e., the use of pesticides, fertilizers, and contaminated water for irrigation [12]. The high availability of toxic and trace elements in the soil of mining areas is due to mining activities, which can pose a significant risk to humans, agricultural land, water bodies, and living organisms. Alternatively, it may affect the food chain, atmospheric quality, infrastructure, aesthetics, and social life of the region [2,13].

Coalmines are an important part of making energy, and almost 27% of the world's economy comes from coal [14]. Open-pit and underground coal exploitations included a phased development in the mines and surrounding rock removal, which have a low concentration of coal (<30%) and high iron sulfide (FeS_2) minerals. Coal mining operations disrupt various parental rock materials, which may release various minerals and toxic elements to the surrounding environment [15]. Furthermore, coal is considered a critical source of energy for maintaining national security in both developed and emerging nations. The majority of industrialized nations, including China, Russia, and the United States, rely heavily on coal energy [16]. The least developed nations, such as Pakistan, lack modern methods for using coal resources for electricity and industrial purposes [17]; however, conventional techniques of coal prospecting have begun in several regions of the country. During typical prospecting procedures, a large volume of coal is wasted and dumped in the adjacent area. According to Hussain et al. [18], a large quantity of coal is lost during coal mining, contaminating local water bodies, agricultural land, food crops, and human health. The present research attempts to investigate the effects of coal waste on the soil in the Makarwal area.

It is now widely understood that coal mineral activities, especially of those metallic minerals, play a greater role in the contamination of water and soils in adjacent areas [19,20]. Therefore, it is expected that coal mining in the study area would certainly have profound environmental impacts on the soils of the study area. To probe the soil contamination, the present study proposes to account for the environmental problems with special emphasis on the soils of the Makarwal coal mining area (Figure 1). In this study, an attempt was made (i) to determine the major and toxic trace elements in coal and soils of the Makarwal coal mining area; (ii) to investigate the environmental impacts (ecological risk) of coal mining on the locality; and (iii) to prepare geochemical concentration maps of various parameters in the soils of the study area.

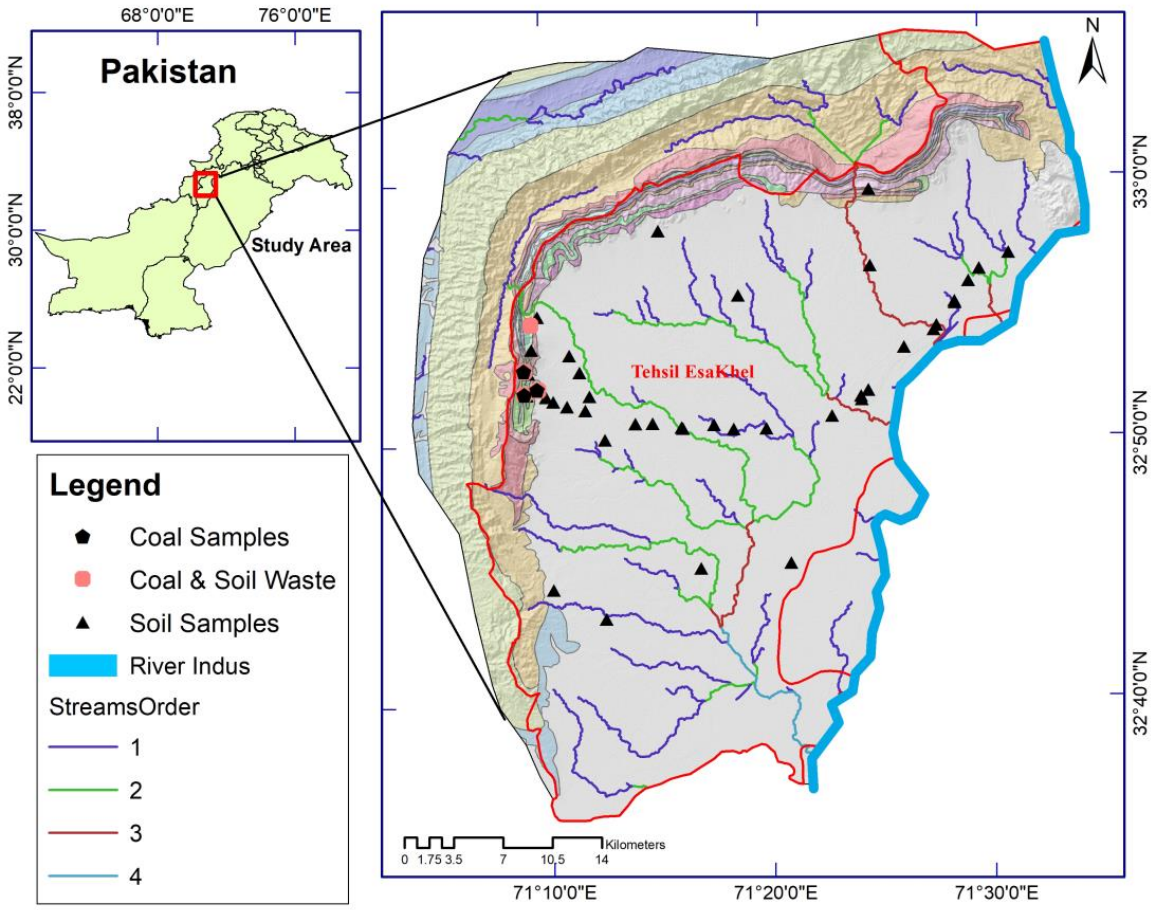

Figure 1. Location map of the study area showing the locations of the coal mines and soil samples.

2. Materials and Methods

2.1. Physiography

The Makarwal coalfield is located in Tehsil Isa Khel, district Mianwali, Punjab, Pakistan, covering an area of about 75 km^2 (Figure 1). According to the national census of 2017, the population of Makarwal is about 70,000. The coal reserves in Makarwal have been estimated at 22 million metric tons, and the annual production during 2014–2015 was 950 hundred metric tons [21].

The Trans-Indus Ranges of Pakistan, which lie west of the Salt Range and the Indus River, are a group of arcuate mountains where distinct ranges include the Surghar, Shinghar, Marwat, and Khisor ranges, located at a distance of about 50 km at the south of Kohat (Figure 1) [22]. The Makarwal coalfield is situated in the Surghar Range, a well-defined series of ridges bounded by a prominent escarpment facing the Indus River [23]. Coal resources in the Trans-Indus mountains were first reported by Wynne [24]. The presence of coal between the Kalabagh and Makarwal areas was first reported by Simpson and Pearson [25]. Gee [26] studied detailed geology and coal resources in the vicinity of Kalabagh and Makarwal, where coal occurs in the steeply dipping Hangu Formation, with the thickness of its bed ranging from 0.5 to 2.0 m.

2.2. Samples Collection

Using a hand auger, a total of 41 soil samples and duplicate samples were taken from different agricultural fields down to a depth of about 0–30 cm at different points to make a single representative sample (Figure 1) [27]. The soil samples were from the Makarwal coalfield located in district Mianwali in May 2021 (coal extraction time). The samples were collected in polythene bags and transferred to the geochemistry laboratory of the National Center of Excellence in Geology (NCEG), University of Peshawar, for further processing.

The representative samples were dried in the air, and all the organic matter was carefully removed. These samples were then ground and screened through a 200-mesh sieve. The pulverized soil samples were stored in airtight polythene bags to avoid contamination [28].

2.3. Experimental Procedures

For the determination of trace elements, each 1 g dried soil sample was taken in a series of clean Teflon beakers and treated with 5 mL of hydrofluoric acid (HF) at a contact temperature of 220 °C. The samples were further treated with 10 mL of Aqua Regia and 20 mL of 2N HCl so that all the elements came into ionic form. The digested contents were then filtered through Whatman Ashless Grade 42 filter paper and diluted to 50 mL. This solution was then used for the determination of toxic trace elements [27,29].

For the determination of major oxides, 0.5 g of each soil sample was treated with HF (10 mL) and perchloric acid ($HClO_4$) (4 mL) for two hours in a series of Teflon beakers. Then, 2 mL of $HClO_4$ was added again to each sample and heated continuously till the paste was obtained. After obtaining the paste, 4 mL of $HClO_4$ was added again to each beaker and heated for a while, and then allowed to cool. Finally, the contents of each beaker were filtered through Whatman ashless grade 42 filter paper in a volumetric flask of 250 mL using deionized water. The digested contents were then used for the determination of major oxides [29,30]. All the trace and major elements were analyzed using the Graphite Furnace Atomic Absorption Spectrophotometer (AAS-A700, Perkin Elmer, Singapore Ltd., USA) at the NCEG, University of Peshawar. All analyses were performed in triplicate, and the accuracy and precision were found within a confidence limit of 90–95%. During this study, the natural background values of Bohn et al. [31] were used as reference values for comparison purposes.

2.4. Pollution Quantification and Risk Assessment

To evaluate the soil pollution and associated health risk in the soil of the Makarwal mining area, various ecological risk methods, namely, the ecological risk index (ERI), contamination factor (CF), geoaccumulation index (I_{geo}), and pollution load index (PLI), were used. These indices allow the assessment of pollution quantification by individual elements and holistic soil quality [32–34].

2.4.1. Contamination Factor

The contamination factor is the ratio obtained between TTEs concentrations in contaminated and reference/background sites and is determined through Equation (1) [35,36].

$$Cf = \frac{C_n}{C_b} \quad (1)$$

where C_n is the concentration of toxic trace metals in contaminated areas and C_b is the concentration of toxic metals in background areas, as suggested by Hussain et al. [29].

2.4.2. Geoaccumulation Index

The geoaccumulation index (I_{geo}) is a geochemical parameter used to evaluate the level of pollution in contaminated soil. The geoaccumulation index can be used as a reference to estimate the extent of pollution and is determined through Equation (2).

$$I_{geo} = Log_2 \left(C_n / 1.5 \times B_n\right) \quad (2)$$

In Equation (2), C_n and B_n are the concentrations of toxic trace elements in the contaminated and background areas, while 1.5 is a possible variation of TTEs in background areas [29]. By assessing the I_{geo} values and soil quality, the degree of contamination was categorized into seven groups [37] (Table 1).

Table 1. Assessment of values, classes, and quality description of the geoaccumulation index.

Class	Values	Soil Quality
0	($I_{geo} \leq 0$)	Uncontaminated
1	($0 < I_{geo} \leq 1$)	Uncontaminated to moderately contaminated
2	($1 < I_{geo} \leq 2$)	Moderately contaminated
3	($2 < I_{geo} \leq 3$)	Moderately to heavily contaminated
4	($3 < I_{geo} \leq 4$)	Heavily contaminated
5	($4 < I_{geo} \leq 5$)	Heavily to extremely contaminated
6	($5 > I_{geo}$)	Extremely contaminated

The highest class (i.e., class 6) reflects 100-fold enrichment relative to the background values.

2.4.3. Pollution Load Index

The pollution load index (PLI) is the integrated extent of contaminants in the target compared to background areas and is determined through Equation (3) [36].

$$PLI = (CF_1 \times CF_2 \times CF_3 \times \ldots CF_n)\frac{1}{n} \quad (3)$$

By assessing the soil quality through PLI, concentrations higher than 1 indicate pollutants in the target areas, while a PLI value less than 1 indicates no pollution in the target area [38,39].

2.4.4. Ecological Risk Assessment

The potential ecological risk index *(ERI)* method was proposed by Hakanson [32] from a sedimentological perspective to assess the characteristics and environmental behavior of heavy metal contaminants in coastal sediments. The main functions of this index are to indicate the contaminants where contamination studies should be prioritized. Ecological risk index (ERI) is the critical measure of soil contamination and risk factor and is calculated through Equation (4).

$$ERI = Tr \times CF \quad (4)$$

where T_r is the toxic response factor. Toxic response values for some of the toxic and trace elements are Cd = 30, Co = 5, Cu = 5, Ni = 5, Pb = 5, Cr = 2, and Zn = 1, as suggested by [32,40].

For the statistical analysis, dendrogram and PCA were determined through SPSS-20 IBM software, while for geospatial distribution, GIS software was used. However, for the graphs, the Origin18 Microsoft version was used.

3. Results and Discussion

3.1. Distribution of Toxic Trace Elements

The concentration ranges of TTEs along with their arithmetic means and standard deviations are presented in Figure 2.

In TTEs, the range of Pb was 6.85–70.55 (average 30.14 ± 13.17), Zn 16.09–94.15 (average 38.33 ± 16.68), Cr 4.4–44.15 (average 20.48 ± 9.00), Ni 15.3–65.15 (average 34.10 ± 9.98), and Cd 0.9–5.95 (average 3.38 ± 1.5) in mg/kg. Among these tips, the concentrations of Pb, Cr, and Cd were higher than those reported by Hussain et al. [18] and Bohn et al. [31], while the concentrations of Ni, Cu, and Zn were higher than those reported by Hussain et al. [18] and Simpson and Pearson [25,31] (Figure 2).

In addition, the average levels of most of the trace elements were found to be several times higher than what the State Environmental Protection Administration of China had set as a limit for cropland [41]. The mean concentration of Zn was lower than the background value, which revealed that there were no anthropogenic sources for Zn in the Makarwal coal mining area. The Zn abundance is mostly associated with sphalerite ore and organic rocks [42]. This indicates that the Makarwal coal mine is deficient in sphalerite and organic minerals. In the study area, the potential source of TTEs was mining smelters, including

mining dumps, tailing dams, extraction dust, loading, and unloading. Similarly, TTEs can be released to agricultural soils through dry deposition, air spreading, rain, local water, leaching of mine dumps, and tailings dams. The mode of occurrence and distribution of TTEs is commonly associated with geomorphological features, living biota, parental rocks and minerals, and climatic variability [43].

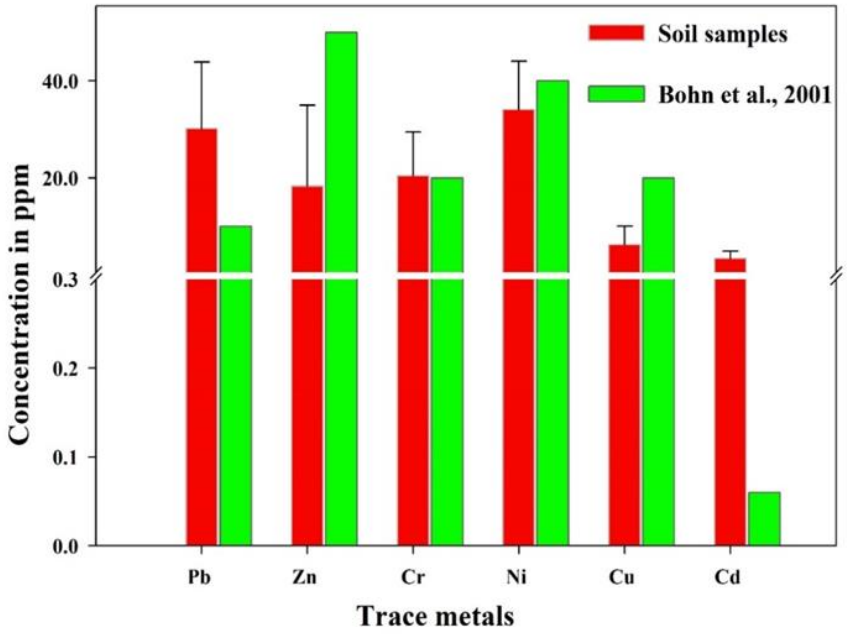

Figure 2. Comparison of mean values of trace element concentrations in the studied soil samples with those of Bohn et al. [31].

The TTE concentration in the Makarwal coalmine-affected region was lower than the global coal-affected regions. The lower concentration in Makarwal may have been due to the young coal mining; however, over time, TTEs in Makarwal will be high enough, as reported in various countries (Table 2). The Zn in Vietnam is commonly associated with weathered geneses, carbonate terrigenous minerals, and hydrothermal materials [44], while in Chinese coal, Zn is attributed to sphalerite ore and organic materials [42] (Table 2).

Table 2. Comparison of toxic trace elements (mg/kg) in coal waste contaminated elsewhere in the world.

Countries	Pb	Zn	Cr	Ni	Cu	Cd
Present study (Pakistan)	30.15	38.33	20.48	34.10	6.24	3.38
China (72 examined mines)	641.3	1163	84.28	106.6	ND	11.00
Iran (3 examine mines)	1002	363.4	ND	ND	88.4	1.49
Spain (16 examined mines)	881.3	465.8	63.2	28.35	120.8	6.59
South Korea (70 examined mines)	111.1	183.2	ND	22.00	79.00	1.99
Vietnam (5 examined mines)	30,635	41,094	1501	2254	271.40	135
India (21 examined mines)	304.7	338.8	1509	1069	63.49	3.82
Chinese Soil Standard [a]	26	74	61	26.9	22.6	0.097
Upper continental Crust [b]	17	71	83	44	25	0.10
Hussain and Luo [42] [c]	7.44	3056	194	83	27.6	0.63

[a]—CEPAC [41], [b]—McLennan [45], [c]—Hussain et al. [18].

The geospatial analysis showed that most of the movement and distribution of TTEs in the Makarwal region were in the middle (Figure 3). However, the concentration of TTEs in the soil affected by coal waste was higher than in the background area. Additionally, the concentration of TTEs was also higher nearby the dumping region as well as on the road at a distance from the coal mining vicinity (Figure 3). The concentration of lead was

high far from the coalmine region, where the rocks mostly belong to Triassic Ceratite and have lead-bearing minerals as compared to the coalmines [46] (Figure 3). Similarly, the concentration of Cd was high in the Makarwal Plain areas, which are considered sinks.

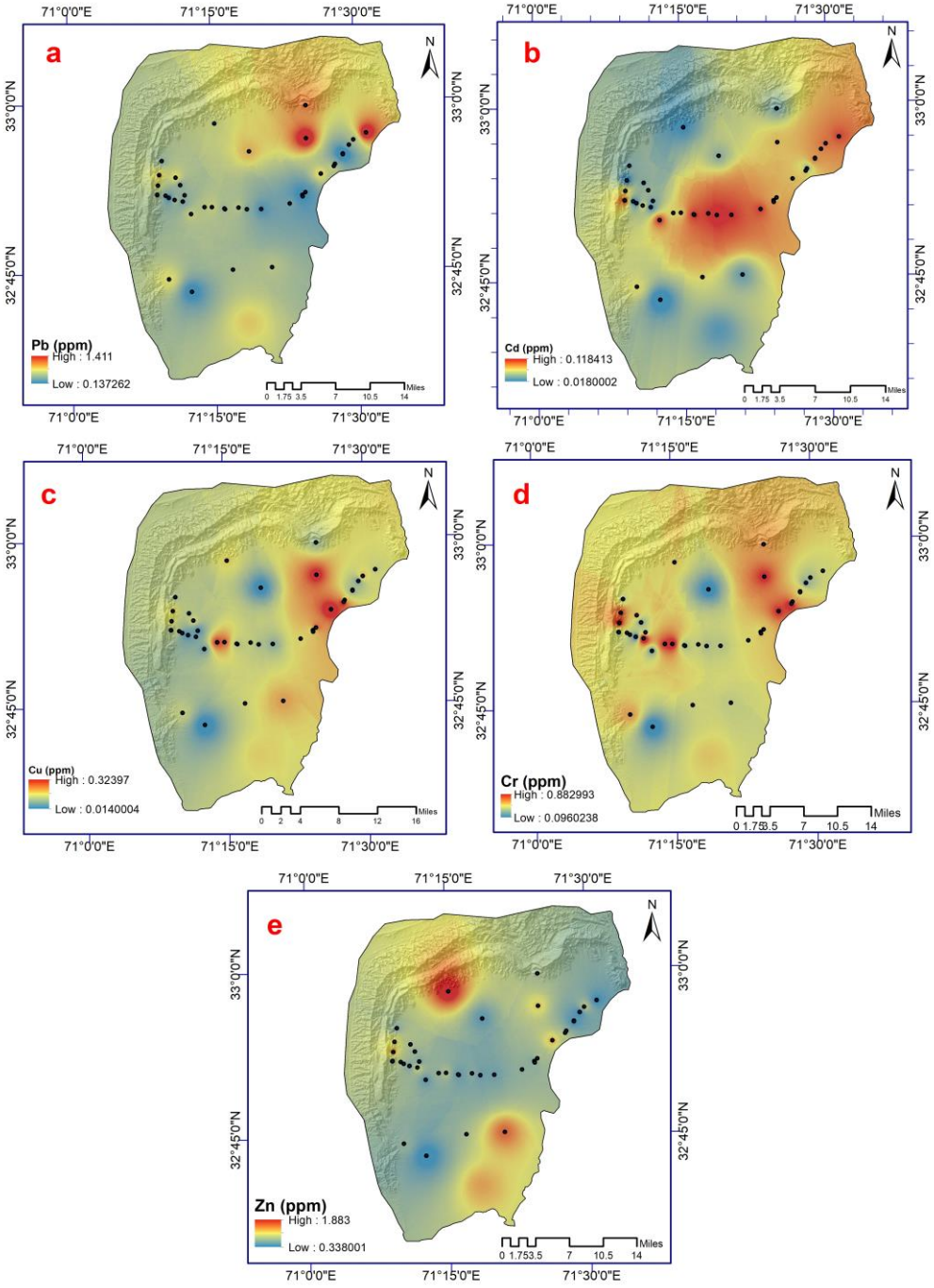

Figure 3. Distribution pattern of trace element concentrations (**a**) Pb, (**b**) Cd, (**c**) Cu, (**d**) Cr, (**e**) Zn in soil samples of the study area.

Moreover, Pearson correlation coefficients between the trace metals were found, which suggests that these metals came from the same place (Table 3). Significant positive correlations ($p < 0.01$) existed between Pb and Ni (r = 0.414), Zn and Cr (r = 0.564), Zn and Ni (r = 0.448), Zn and Cu (r = 0.539), Cr and Ni (r = 0.743), Cr and Cu (r = 0.70), and Ni and Cu (r = 0.853). However, relatively weak positive relationships with a significance of $p < 0.05$ were found between Pb and Zn (r = 0.366) and Pb and Cr (r = 0.71). Interelemental relationships could provide interesting information on the sources and pathways of the

metals, i.e., correlations between Pb and Zn indicated the possibility of a common source that was derived from waste minerals and tailings of lead and zinc ores [47].

Table 3. Pearson correlation analysis of trace elements in soil samples.

Elements	Pb	Zn	Cr	Ni	Cu	Cd
Pb	1.00					
Zn	0.366 *	1.00				
Cr	0.371 *	0.564 **	1.00			
Ni	0.414 **	0.448 **	0.743 **	1.00		
Cu	0.387 **	0.559 **	0.701 **	0.853 **	1.00	
Cd	0.042	−0.274	−0.127	0.222	0.121	1.00

* Correlation is significant at the 0.05 level (2-tailed). ** Correlation is significant at the 0.01 level (2-tailed).

However, to explore the mode of occurrence and elemental geochemistry (i.e., controlling elemental concentration), factor analysis (FA) and hierarchical cluster analysis (HCA) were used. Factor analysis is used to infer the hypothetical source of trace metals (natural or anthropogenic), their mode of occurrence, and controlling factors [48]. It was performed by varimax rotation to minimize the number of variables with high loading on each component and, therefore, facilitate the interpretation of FA results. This technique clusters variables into groups such that variables belonging to one group are highly correlated with one another. According to FA, two principal components were extracted cumulatively and accounted for 53% and 21% of the total variance of the trace metal concentrations in F1 and F2, respectively (Table 4).

Table 4. Results of principal component analysis of the soil samples of the Makarwal region.

TTEs	F1	F2
Pb	0.587	0.040
Zn	0.722	−0.443
Cr	0.864	−0.131
Ni	0.892	0.288
Cu	0.900	0.158
Cd	0.011	0.954
Eigen	3.206	1.247
% variance	53.437	20.777
Cumulative	53.437	74.214

The total variance was explained by F1, with positive loadings of 0.722, 0.864, 0.892, and 0.900 for Zn, Cr, and Ni, respectively, while F2 accounted for 20.78% of the total variance, with a positive loading of 0.954 for Cd, which may be associated with carbonates and sulfides (Table 3). The heavily loaded elements in F1 may be associated with the clay minerals dolomite and calcite, which were also reported by Danilchik and Shah [46]. Hence, the FA plays a significant role in explaining metal contamination and controlling factors in the study area. Additionally, principal component coefficients greater than 0.70 are considered highly significant [49].

The FA results were further supported by hierarchical analysis. The clusters can be distinguished in the dendrogram-analyzed parameters with the average linkage method and the squared Euclidean distance as a similarity measure (Figure 4). Factor 1 was loaded with elements, namely, Cu and Cd, as the variability of these elements was controlled by parent rocks. However, factor 2 consists of Pb, Ni, Zn, and Cr, which were identified as contaminants derived from parent rock material characterized by sand and limestone. The result of the present study is consistent with that of Danilchik and Shah [46]. The loaded element's contents in F2 were similar to cluster 2; i.e., Pb, Ni, Cr, and Zn, while cluster 1′s load was similar to F1 (Figure 4), which proved that the contamination in the surrounding areas is associated with the parental rock of the Makarwal coalfield.

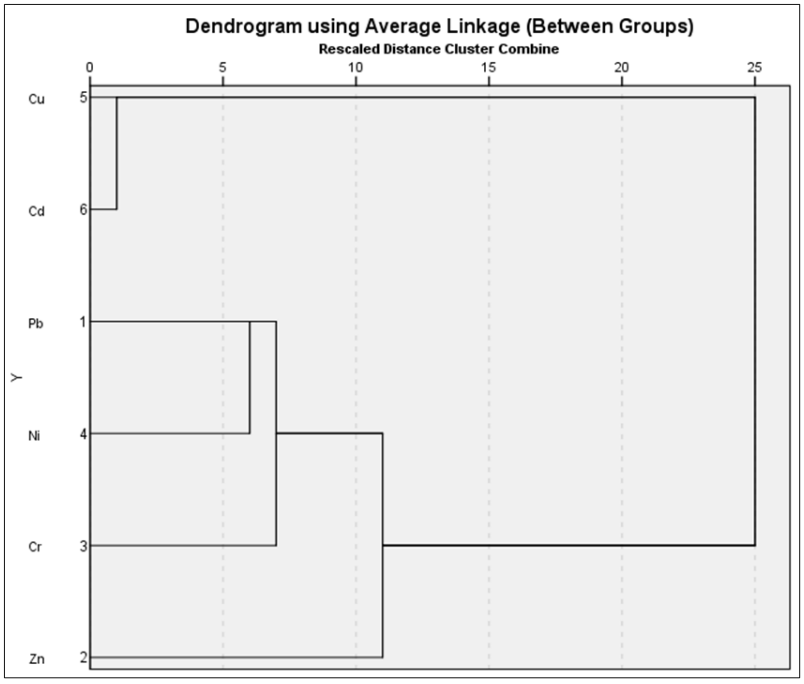

Figure 4. Dendrogram obtained by hierarchical cluster analysis of trace elements in soil samples of the study area.

3.2. Major Oxides Distribution

The concentrations of CaO in the soil samples of the study area were 0.69% to 23.29%. This concentration is multifold higher than that of the normal soil (0.51%) of the USDA [50], Chinese soil standard (CSS) of 1.54% [51], and the upper continental crust (UCC) of 3.0% [45], which is considered in Pakistan as the background value (Figure 5).

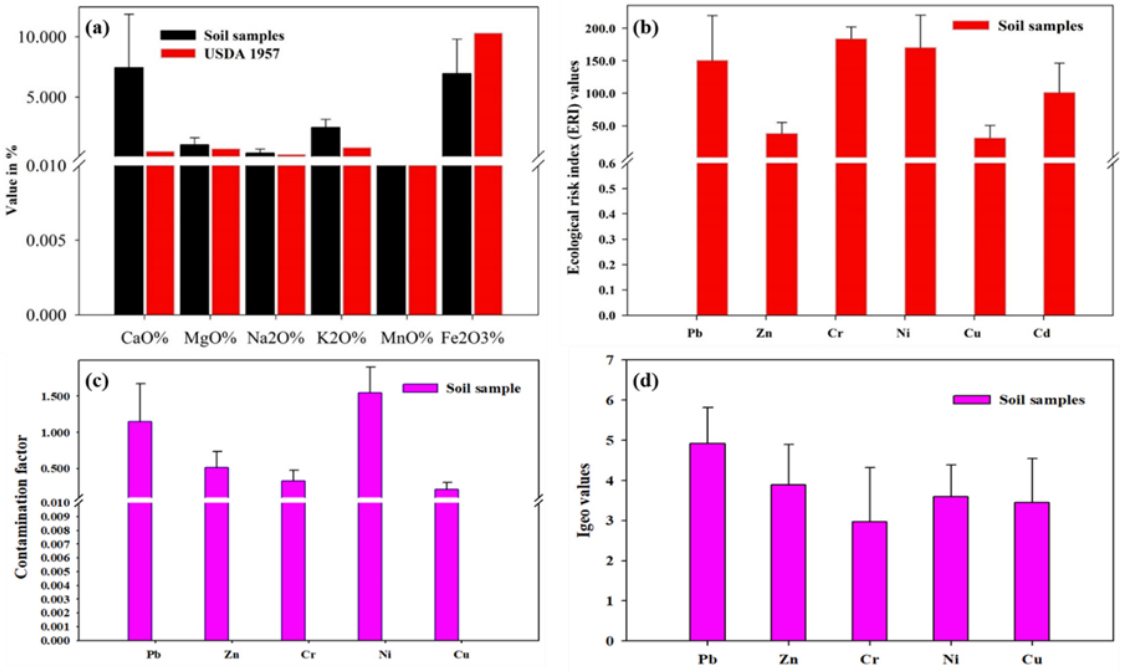

Figure 5. (**a**) A comparison of major oxides with the normal soil concentration of USDA [50]; (**b**) potential ecological risk of trace elements in Makarwal soil; (**c**) contamination factor of Makarwal coal-mining-contaminated soil; (**d**) geoaccumulation index of Makarwal coal soil.

The distribution map showed that CaO in the soil in the northern and southwestern parts was comparatively more enriched as compared to the other areas (Figure 6). The high concentration in northern and southern parts is attributed to the Paleocene coal-bearing strata of the Makarwal coalfield. Calcium in the soil is normally contributed by calcite and dolomite, which are the major constituents of limestone. However, the primary source of Ca in the Earth's crust is feldspar, while gypsum and limestone are the secondary sources [52,53].

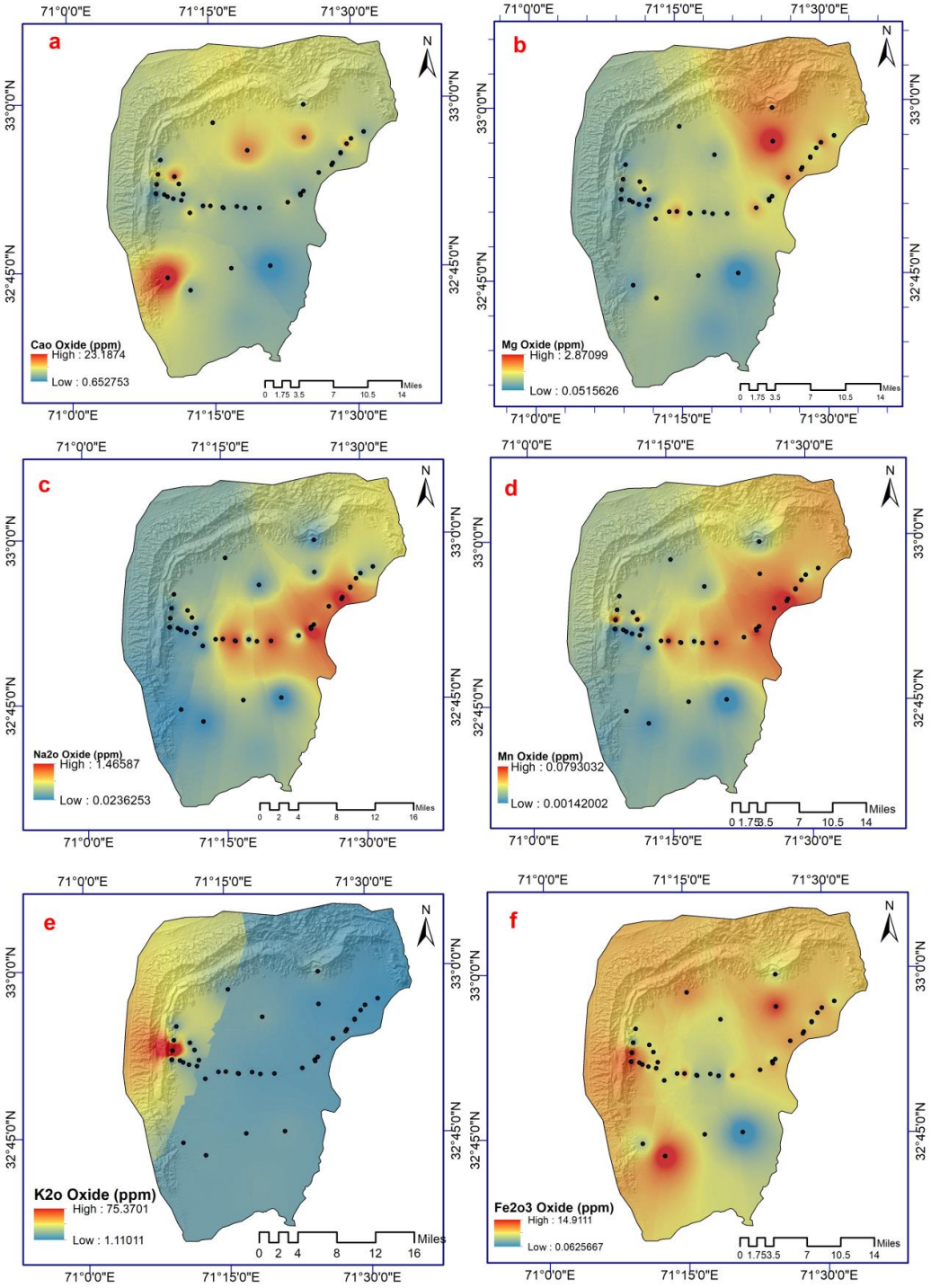

Figure 6. Concentration distribution maps of the major oxides (**a**) CaO, (**b**) MgO, (**c**) Na_2O, (**d**) MnO, (**e**) K_2O, (**f**) Fe_2O_3 in the soil samples of the study area.

The concentration of MgO in the Makarwal region was 0.05–2.87% with an average amount of 1.05%, which was comparably higher than the CSS of 0.78% [51] (Figure 5). The MgO concentration in the studied soils also exceeds that of normal soils, i.e., 0.71% [50] (Figure 5a). The concentration distribution of MgO in the study area showed that the soil in the northeastern part of the study area was more enriched as compared to the other areas (Figure 6b). The increase in MgO concentration in the soils is normally attributed to the weathering of dolomites and ultramafic rocks in the adjacent areas [31].

The concentration of Na_2O in soil samples from the study area ranged from 0.02 to 1.47%, which was higher than that of normal US soil [50] (Figure 5a). A concentration distribution map of Na_2O shows that the soils of the central parts of the study area are relatively enriched in Na_2O as compared to the boundary areas of the Makarwal coalfield (Figure 6c). Sodium normally contributes to the soils due to the weathering of igneous and sedimentary rocks in the adjacent areas [54]. The high concentration in the center is due to the mobility of contamination to the central part and accumulation in that environment.

Similarly, the concentration of MnO in the soil samples of the study area was negligible, i.e., 0.00% to 0.08%, which was similar to that of the normal soil [31], i.e., 0.030%. The distribution of MnO in the soils of the study area shows that MnO is relatively high in the northeastern parts of the study area, which is possibly associated with the weathering of mineralized rocks (Figure 6d). Manganese is a common trace element that generally contributes to the soils by the weathering of adjacent mafic rocks [55].

The K_2O contents in the soil samples of the study area were 1.1 to 3.4%. This indicates that the studied soils have a greater concentration of K_2O as compared to the normal soils of the USDA [50], i.e., 0.81%. A concentration distribution map shows that the soils of the western parts are relatively enriched in K_2O (Figure 6e). Potassium generally contributes to the soils due to the weathering of the minerals such as feldspar, illite, and mica, which are abundantly present in the adjacent rocks [52,53].

The concentrations of Fe_2O_3 were 0.06–14.53%, with an average of 6.25% (Figure 5a). The studied soils have a lower average concentration of Fe_2O_3 as compared to the normal soils of the USDA [50] (10.11%); however, the concentration distribution map indicates that the soils of the northeastern and southwestern parts of the study area have a relatively higher amount of Fe_2O_3 (Figure 6f). This high concentration of Fe_2O_3 is attributed to the mineralized rock strata. The concentration of Fe_2O_3 in the Makarwal regions was also higher than that of Hussain et al. [18], i.e., 3.06%, CSS (2.94%) [51], and UCC (3.5%) [45].

3.3. Assessment of Potential Ecological Risk Index for Soil

The ecological risk index (ERI) is widely used to evaluate the potential ecological risk caused by pollutants, such as trace metals, and their impacts on the ecological system [18,27,56], but one problem with this method is that it is very subjective and does not take into account how different trace metals interact with each other [57]. The ERI assessment considers the toxicity effect of an element alongside the measured concentration of soil in comparison with the reference value of the element in the Earth's crust. The ERI results of the trace elements were plotted in Figure 5b. The single trace element contamination index highlights that Cd, Pb, Ni, and Cr pose a high risk to human health and the ecosystem. The distribution pattern of Pb shows that it was generally found in all the sampled areas, and its potential ecological risk indices are the same as those of the general potential ecological risk for all trace metals (Figure 5b). The potential ecological risk indices for TTEs decrease in the following sequence: Cr > Ni > Pb > Cd > Cu > Zn. The sources of trace metal pollution in the soil samples were influenced by many factors, including natural and anthropogenic ones, as also reported by Hussain et al. [18] and Chifflet et al. [58]. Natural factors can be, for example, the weathering processes of rocks and minerals [59–61], while in many cases, the anthropogenic factors can include several activities, such as urban, agricultural, industrial, mining, or transportation [2,9,11,61–65].

The indices, such as the contamination factor (CF), were implemented to gauge the level of trace metal pollution in the rural environment of mining areas in Makarwal. Among

all the trace metals, Ni has the highest CF value (1.54) followed by Pb (1.14), which could be considered as moderate to high contamination (1 < CF < 3) in the area (Figure 5c). However, Zn, Cr, and Cu exhibit low to moderate contamination (Figure 5c). The combined pollution load index was extracted from the contamination factor, which exhibits a decreasing trend for trace elements as follows: Ni > Pb > Zn > Cr > Cu (Figure 5c).

Figure 5d shows a graph of the geoaccumulation indices (I_{geo}) for toxic trace metals in soil samples from the Makarwal coal mine area. It is clear from the figure that the mean I_{geo} trend for toxic trace metals follows a decreasing order, i.e., Pb > Zn > Ni > Cu > Cr (Figure 5d). This elemental concentration in the studied soil sample suggests that the soils of the area may be moderately to severely polluted by Pb, Zn, and Ni and moderately polluted by Cr and Cu (Figure 5d).

4. Conclusions

The present study determined that the contamination in the soil of the Makarwal region was high and was attributed to coal-mining-associated minerals. In the Makarwal region, the soil has a high concentration of toxic race elements, namely, Ni, Pb, Cd, Cr, and Cu, compared to the recommended guideline values of CSS, UCC, and USDA. These trace elements, based on highest to lowest mean concentration, were Ni > Pb > Cd > Cu > Cr > Zn. The factor analysis (FA) indicates that two components were obtained, showing 70.38% and 74.21% of total variability for coal and soil, respectively. The potential ecological risk of toxic trace metals was Pb > Cr > Ni > Cd > Cu > Zn. The F2 consists of Pb, Ni, Zn, and Cr, which were identified as contaminants derived from parent rock material characterized by sand and limestone, while the variability of the F1 elements, namely, Cu and Cd, is controlled by the parent rocks. The geospatial distribution revealed that the concentration of TTEs was higher in the center while reducing the far-off distance from the center of the study areas. The high concentration in the northern and southern parts is attributed to the Paleocene coal-bearing strata of the Makarwal coalfield. Ca, Mg, and TTEs in the soil are normally contributed by coal, particularly calcite and dolomite strata, which are the major constituents of limestone. Not only do coal mines contaminate the surrounding soil, but existing geological strata's weathering, erosion of host rocks (limestone, dolomite, and shale), and surface runoff also disrupt the Makarwal soil, which may affect food crops and humans. This study recommends applying sustainable coal mining techniques, which will be helpful to limit soil contamination and health risk.

Author Contributions: Conceptualization, L.A. and S.A.; methodology, L.A, S.A., S.A.K., R.H., S.R. and M.T.S.; software, L.A, S.A., S.A.K., R.H., S.R. and M.T.S.; validation, L.A, S.A., S.A.K., R.H., S.R., M.T.S., H.T.J. and G.K.; formal analysis, S.A., S.A.K., R.H. and S.R.; investigation, L.A, S.A., S.A.K., R.H., S.R., M.T.S., H.T.J., G.K., G.D.B. and H.D.S.; resources, L.A., S.A., R.H. and S.A.K.; data curation, L.A., S.A., R.H. and S.A.K.; writing—original draft preparation, L.A., R.H., M.T.S. and S.A.K.; writing—review and editing, L.A, S.A., S.A.K., R.H., S.R., M.T.S., H.T.J., G.K., G.D.B. and H.D.S.; visualization, R.H., L.A., M.T.S. and S.R.; supervision, S.A.; project administration, G.K. and H.T.J.; funding acquisition, G.D.B. and H.D.S. All authors have read and agreed to the published version of the manuscript.

Funding: This research received no external funding.

Data Availability Statement: The data used in this work are available on request to the corresponding author(s).

Acknowledgments: National Centre of Excellence in Geology, University of Peshawar, College of Earth and Environmental Sciences, University of the Punjab, Lahore, Pakistan, is highly acknowledged for providing laboratory facilities, financial support for fieldwork, and encouragement during the entire period of research.

Conflicts of Interest: The authors declare no conflict of interest.

References

1. Kirby, B.; Vengadajellum, C.; Burton, S.; Cowan, D. Coal, coal mines and spoil heaps. In *Handbook of Hydrocarbon and Lipid Microbiology*; Springer: Berlin/Heidelberg, Germany, 2010.
2. Janjuhah, H.T.; Ishfaque, M.; Mehmood, M.I.; Kontakiotis, G.; Shahzad, S.M.; Zarkogiannis, S.D. Integrated Underground Mining Hazard Assessment, Management, Environmental Monitoring, and Policy Control in Pakistan. *Sustainability* **2021**, *13*, 13505. [CrossRef]
3. Rodríguez-Pacheco, R.; García, G.; Caparrós-Ríos, A.V.; Robles-Arenas, V.; García-García, C.; Millán, R.; Pérez-Sanz, A.; Alcolea-Rubio, L.A. Mineralogy, Geochemistry and Environmental Hazards of Different Types of Mining Waste from a Former Mediterranean Metal Mining Area. *Land* **2023**, *12*, 499. [CrossRef]
4. Belanović Simić, S.; Miljković, P.; Baumgertel, A.; Lukić, S.; Ljubičić, J.; Čakmak, D. Environmental and Health Risk Assessment Due to Potentially Toxic Elements in Soil near Former Antimony Mine in Western Serbia. *Land* **2023**, *12*, 421. [CrossRef]
5. Somoano, M.D. Minimization of Hg and trace elements during coal combustion and gasification processes. In *New Trends in Coal Conversion*; Elsevier: Amsterdam, The Netherlands, 2019; pp. 59–88.
6. Finkleman, D.; Santiago, J.; Alfano, S.; Vallado, D. Introduction to Data Fusion and Applications in Astrodynamics. *Multisens. Fusion* **2002**, *70*, 657–671.
7. Mohanty, A.K.; Lingaswamy, M.; Rao, V.G.; Sankaran, S. Impact of acid mine drainage and hydrogeochemical studies in a part of Rajrappa coal mining area of Ramgarh District, Jharkhand State of India. *Groundw. Sustain. Dev.* **2018**, *7*, 164–175. [CrossRef]
8. Wang, Y.; Wang, R.; Fan, L.; Chen, T.; Bai, Y.; Yu, Q.; Liu, Y. Assessment of multiple exposure to chemical elements and health risks among residents near Huodehong lead-zinc mining area in Yunnan, Southwest China. *Chemosphere* **2017**, *174*, 613–627. [CrossRef]
9. Makri, P.; Stathopoulou, E.; Hermides, D.; Kontakiotis, G.; Zarkogiannis, S.D.; Skilodimou, H.D.; Bathrellos, G.D.; Antonarakou, A.; Scoullos, M. The Environmental Impact of a Complex Hydrogeological System on Hydrocarbon-Pollutants' Natural Attenuation: The Case of the Coastal Aquifers in Eleusis, West Attica, Greece. *J. Mar. Sci. Eng.* **2020**, *8*, 18. [CrossRef]
10. Hermides, D.; Makri, P.; Kontakiotis, G.; Antonarakou, A. Advances in the Coastal and Submarine Groundwater Processes: Controls and Environmental Impact on the Thriassion Plain and Eleusis Gulf (Attica, Greece). *J. Mar. Sci. Eng.* **2020**, *8*, 944. [CrossRef]
11. Makri, P.; Hermides, D.; Kontakiotis, G.; Zarkogiannis, S.D.; Besiou, E.; Janjuhah, H.T.; Antonarakou, A. Integrated Ecological Assessment of Heavily Polluted Sedimentary Basin within the Broader Industrialized Area of Thriassion Plain (Western Attica, Greece). *Water* **2022**, *14*, 382. [CrossRef]
12. Komnitsas, K.; Modis, K. Soil risk assessment of As and Zn contamination in a coal mining region using geostatisretics. *Sci. Total Environ.* **2006**, *371*, 190–196. [CrossRef]
13. Li, Z.; Ma, Z.; van der Kuijp, T.J.; Yuan, Z.; Huang, L. A review of soil heavy metal pollution from mines in China: Pollution and health risk assessment. *Sci. Total Environ.* **2014**, *468*, 843–853. [CrossRef]
14. Bhuiyan, M.A.; Parvez, L.; Islam, M.; Dampare, S.B.; Suzuki, S. Heavy metal pollution of coal mine-affected agricultural soils in the northern part of Bangladesh. *J. Hazard. Mater.* **2010**, *173*, 384–392. [CrossRef]
15. Swaine, D.J.; Goodarzi, F. General introduction. In *Environmental Aspects of Trace Elements in Coal*; Springer: Berlin/Heidelberg, Germany, 1995; pp. 1–4.
16. Asif, M.; Muneer, T. Energy supply, its demand and security issues for developed and emerging economies. *Renew. Sustain. Energy Rev.* **2007**, *11*, 1388–1413. [CrossRef]
17. Abbasi, S.A.; Harijan, K.; Memon, Z.A.; Shaikh, F.; Mirjat, N.H. Is Coal Power Generation a Sustainable Solution for Energy Needs of Pakistan: A Delphi-SWOT Paradigm? *Int. J. Energy Econ. Policy* **2021**, *11*, 308. [CrossRef]
18. Hussain, R.; Luo, K.; Liang, H.; Hong, X. Impact of the coal mining-contaminated soil on the food safety in Shaanxi, China. *Environ. Geochem. Health* **2019**, *41*, 1521–1544. [CrossRef]
19. Zhuang, W.; Gao, X. Integrated assessment of heavy metal pollution in the surface sediments of the Laizhou Bay and the coastal waters of the Zhangzi Island, China: Comparison among typical marine sediment quality indices. *PLoS ONE* **2014**, *9*, e94145. [CrossRef]
20. Sun, L.; Guo, D.; Liu, K.; Meng, H.; Zheng, Y.; Yuan, F.; Zhu, G. Levels, sources, and spatial distribution of heavy metals in soils from a typical coal industrial city of Tangshan, China. *CATENA* **2019**, *175*, 101–109. [CrossRef]
21. Malkani, M.S.; Mahmood, Z. Coal Resources of Pakistan: Entry of new coalfields. *Geol. Surv. Pak. Inf. Release* **2017**, *980*, 1–28.
22. Blisniuk, P.M. *Tectonic Evolution of the NW-Himalayan Thrust Front: The Trans-Indus Ranges, Northern Pakistan*; Dartmouth College: Hanover, NH, USA, 1996.
23. Ali, A. *Structural Analysis of the Trans-Indus Ranges: Implications for the Hydrocarbon Potential of the NW Himalayas, Pakistan*; National Centre of Excellence in Geology University of Peshawar: Pakhtunkhwa, Pakistan, 2010.
24. Wynne, A. On the trans-indus extension of the Punjab Salt Range. *Geol. Surv. India Mem.* **1880**, *17*, 1–95.
25. Simpson, R.; Pearson, K. Report on certain enteric fever inoculation statistics. *Br. Med. J.* **1904**, *2*, 1243–1246.
26. Gee, G. The photopolymerisation of butadiene. *Trans. Faraday Soc.* **1938**, *34*, 712–728. [CrossRef]
27. Hussain, R.; Khattak, S.A.; Sattar, S.; Ali, L.; Ullah, Z.; Muhammad, N. Evaluation of the contaminated soil and its impacts on Tobacco (*Nicotiana tabacum* L.) crops in Swabi, Pakistan. *J. Himal. Earth Sci.* **2020**, *53*, 34–48.
28. Du, Y.; Luo, K.; Ni, R.; Hussain, R. Selenium and hazardous elements distribution in plant–soil–water system and human health risk assessment of Lower Cambrian, Southern Shaanxi, China. *Environ. Geochem. Health* **2018**, *40*, 2049–2069. [CrossRef] [PubMed]

29. Hussain, R.; Khattak, S.A.; Shah, M.T.; Ali, L. Multistatistical approaches for environmental geochemical assessment of pollutants in soils of Gadoon Amazai Industrial Estate, Pakistan. *J. Soils Sediments* **2015**, *15*, 1119–1129. [CrossRef]
30. Khan, S.; Rehman, S.; Khan, A.Z.; Khan, M.A.; Shah, M.T. Soil and vegetables enrichment with heavy metals from geological sources in Gilgit, northern Pakistan. *Ecotoxicol. Environ. Saf.* **2010**, *73*, 1820–1827. [CrossRef]
31. Bohn, H.; McNeal, B.; O'Connor, G. *Soil Chemistry*, 3rd ed.; John Wiley and Sons: New York, NY, USA, 2001; Volume 303, pp. 48–66.
32. Hakanson, L. An ecological risk index for aquatic pollution control. A sedimentological approach. *Water Res.* **1980**, *14*, 975–1001. [CrossRef]
33. Ho, H.H.; Swennen, R.; Van Damme, A. Distribution and Contamination Status of Heavy Metals in Estuarine Sediments Near Cua Ong Harbor, Ha Long Bay, Vietnam. *Geol. Belg.* **2010**, *13/1-2*, 37–47.
34. Hussain, R.; Luo, K. Geochemical valuation and intake of F, As, and Se in coal wastes contaminated areas and their potential impacts on local inhabitants, Shaanxi China. *Environ. Geochem. Health* **2018**, *40*, 2667–2683. [CrossRef]
35. Rashed, M. Monitoring of contaminated toxic and heavy metals, from mine tailings through age accumulation, in soil and some wild plants at Southeast Egypt. *J. Hazard. Mater.* **2010**, *178*, 739–746. [CrossRef]
36. Muhammad, S.; Shah, M.T.; Khan, S. Heavy metal concentrations in soil and wild plants growing around Pb–Zn sulfide terrain in the Kohistan region, northern Pakistan. *Microchem. J.* **2011**, *99*, 67–75. [CrossRef]
37. Muller, G. Index of geoaccumulation in sediments of the Rhine River. *Geojournal* **1969**, *2*, 108–118.
38. Atgin, R.S.; El-Agha, O.; Zararsız, A.; Kocataş, A.; Parlak, H.; Tuncel, G. Investigation of the sediment pollution in Izmir Bay: Trace elements. *Spectrochim. Acta Part B At. Spectrosc.* **2000**, *55*, 1151–1164. [CrossRef]
39. Hu, W.; Chen, Y.; Huang, B.; Niedermann, S. Health risk assessment of heavy metals in soils and vegetables from a typical greenhouse vegetable production system in China. *Hum. Ecol. Risk Assess. Int. J.* **2014**, *20*, 1264–1280. [CrossRef]
40. Håkanson, L.; Nilsson, Å.; Andersson, T. Mercury in fish in Swedish lakes. *Environ. Pollut.* **1988**, *49*, 145–162. [CrossRef]
41. CEPAC. China National Environmental Monitoring Center. A Brief Discussion on National Ambient Air Quality Forecast and Early Warning System. Available online: http://www.cnemc.cn/en/ (accessed on 1 March 2023).
42. Hussain, R.; Luo, K. Geochemical Evaluation of Enrichment of Rare-Earth and Critical Elements in Coal Wastes from Jurassic and Permo-Carboniferous Coals in Ordos Basin, China. *Nat. Resour. Res.* **2020**, *29*, 1731–1754. [CrossRef]
43. Centeno, J.A.; Finkelman, R.B.; Selinus, O. Medical geology: Impacts of the natural environment on public health. *Geosciences* **2016**, *6*, 8. [CrossRef]
44. Khoi, N.N. Mineral resources potential of Vietnam and current state of mining activity. *Appl. Environ. Res.* **2014**, *36*, 37–46. [CrossRef]
45. McLennan, S.M. Relationships between the trace element composition of sedimentary rocks and upper continental crust. *Geochem. Geophys. Geosystems* **2001**, *2*, 2000GC000109. [CrossRef]
46. Danilchik, W.; Shah, S.M. Stratigraphy and coal resources of the Makarwal area, Trans-Indus mountains, Mianwali district, Pakistan. *United States Geol. Surv. Prof. Pap.* **1987**, *75*, 1341.
47. Ma, L.; Sun, J.; Yang, Z.; Wang, L. Heavy metal contamination of agricultural soils affected by mining activities around the Ganxi River in Chenzhou, Southern China. *Environ. Monit. Assess.* **2015**, *187*, 731. [CrossRef]
48. Hussain, R.; Wei, C.; Luo, K. Hydrogeochemical characteristics, source identification and health risks of surface water and groundwater in mining and non-mining areas of Handan, China. *Environ. Earth Sci.* **2019**, *78*, 402. [CrossRef]
49. Montazeri, A.; Harirchi, A.M.; Shariati, M.; Garmaroudi, G.; Ebadi, M.; Fateh, A. The 12-item General Health Questionnaire (GHQ-12): Translation and validation study of the Iranian version. *Health Qual. Life Outcomes* **2003**, *1*, 66. [CrossRef]
50. USDA. Soil. In *Year Book of Agriculture*; The United States Department of Agriculture, Amazon Book Club: Washington, DC, USA, 1957.
51. *GB 15618-1995*; Environmental quality standard for soils. State Environmental Protection Administration of China (SEPAC): Beijing, China, 1995.
52. Bozkaya, Ö.; Günal-Türkmenoğlu, A.; Göncüoğlu, M.C.; Okuyucu, C. Geological, mineralogical and geochemical characteristics of Mississippian K-bentonites from southern Turkey: A correlation with coeval tephras from Gondwana-derived terranes. *J. Afr. Earth Sci.* **2021**, *181*, 104258. [CrossRef]
53. Dou, W.; Liu, L.; Wu, K.; Xu, Z.; Feng, X. Diagenesis of tight oil sand reservoirs: Upper Triassic tight sandstones of Yanchang Formation in Ordos Basin, China. *Geol. J.* **2018**, *53*, 707–724. [CrossRef]
54. Wang, T.; Cao, J.; Carroll, A.R.; Zhi, D.; Tang, Y.; Wang, X.; Li, Y. Oldest preserved sodium carbonate evaporite: Late Paleozoic Fengcheng Formation, Junggar Basin, NW China. *Bulletin* **2021**, *133*, 1465–1482. [CrossRef]
55. Sasmaz, A.; Zagnitko, V.M.; Sasmaz, B. Major, trace and rare earth element (REE) geochemistry of the Oligocene stratiform manganese oxide-hydroxide deposits in the Nikopol, Ukraine. *Ore Geol. Rev.* **2020**, *126*, 103772. [CrossRef]
56. Sulaiman, M.; Salawu, K.; Barambu, A. Assessment of concentrations and ecological risk of heavy metals at resident and remediated soils of uncontrolled mining site at Dareta Village, Zamfara, Nigeria. *J. Appl. Sci. Environ. Manag.* **2019**, *23*, 187–193. [CrossRef]
57. Bali, A.S.; Sidhu, G.P.S. Heavy metal contamination indices and ecological risk assessment index to assess metal pollution status in different soils. In *Heavy Metals in the Environment*; Elsevier: Amsterdam, The Netherlands, 2021; pp. 87–98.

58. Chifflet, S.; Amouroux, D.; Bérail, S.; Barre, J.; Van, T.C.; Baltrons, O.; Brune, J.; Dufour, A.; Guinot, B.; Mari, X. Origins and discrimination between local and regional atmospheric pollution in Haiphong (Vietnam), based on metal (loid) concentrations and lead isotopic ratios in PM 10. *Environ. Sci. Pollut. Res.* **2018**, *25*, 26653–26668. [CrossRef]
59. Alexakis, D.E.; Bathrellos, G.D.; Skilodimou, H.D.; Gamvroula, D.E. Spatial Distribution and Evaluation of Arsenic and Zinc Content in the Soil of a Karst Landscape. *Sustainability* **2021**, *13*, 6976. [CrossRef]
60. Bathrellos, G.D.; Skilodimou, H.D. Land Use Planning for Natural Hazards. *Land* **2019**, *8*, 128. [CrossRef]
61. Khan, U.; Janjuhah, H.T.; Kontakiotis, G.; Rehman, A.; Zarkogiannis, S.D. Natural Processes and Anthropogenic Activity in the Indus River Sedimentary Environment in Pakistan: A Critical Review. *J. Mar. Sci. Eng.* **2021**, *9*, 1109. [CrossRef]
62. Golia, E.E.; Papadimou, S.G.; Cavalaris, C.; Tsiropoulos, N.G. Level of Contamination Assessment of Potentially Toxic Elements in the Urban Soils of Volos City (Central Greece). *Sustainability* **2021**, *13*, 2029. [CrossRef]
63. Alexakis, D.E.; Bathrellos, G.D.; Skilodimou, H.D.; Gamvroula, D.E. Land Suitability Mapping Using Geochemical and Spatial Analysis Methods. *Appl. Sci.* **2021**, *11*, 5404. [CrossRef]
64. Dimirkou, A.; Ioannou, Z.; Golia, E.E.; Danalatos, N.; Mitsios, I.K. Sorption of Cadmium and Arsenic by Goethite and Clinoptilolite. *Commun. Soil Sci. Plant Anal.* **2009**, *40*, 259–272. [CrossRef]
65. Haq, N.U.; Kontakiotis, G.; Janjuhah, H.T.; Rahman, F.; Tabassum, I.; Khan, U.; Khan, J.; Ahmad, Z.; Jamal, N. Environmental Risk Assessment in the Hindu Kush Himalayan Mountains of Northern Pakistan: Palas Valley, Kohistan. *Sustainability* **2022**, *14*, 16679. [CrossRef]

Disclaimer/Publisher's Note: The statements, opinions and data contained in all publications are solely those of the individual author(s) and contributor(s) and not of MDPI and/or the editor(s). MDPI and/or the editor(s) disclaim responsibility for any injury to people or property resulting from any ideas, methods, instructions or products referred to in the content.